Chemistry Europe
European Chemical Societies Publishing

d/f-Polypnictides Derived by Non-Classical Ln^{2+} Compounds: Synthesis, Small Molecule Activation and Optical Properties

Niklas Reinfandt,[a] Nadine Michenfelder,[b] Christoph Schoo,[a] Ravi Yadav,[a] Stephan Reichl,[c] Sergey N. Konchenko,[d] Andreas N. Unterreiner,[b] Manfred Scheer,[c] and Peter W. Roesky*[a]

Abstract: Reduction chemistry induced by divalent lanthanides has been primarily focused on samarium so far. In light of the rich physical properties of the lanthanides, this limitation to one element is a drawback. Since molecular divalent compounds of almost all lanthanides have been available for some time, we used one known and two new non-classical reducing agents of the early lanthanides to establish a sophisticated reduction chemistry. As a result, six new d/f-polyphosphides or d/f-polyarsenides, [K(18-crown-6)] $[Cp''_2Ln(E_5)FeCp^*]$ (Ln = La, Ce, Nd; E = P, As) were obtained. Their reactivity was studied by activation of P_4, resulting in a selective expansion of the P_5 rings. The obtained compounds [K(18-crown-6)] $[Cp''_2Ln(P_7)FeCp^*]$ (Ln = La, Nd) are the first examples of an activation of P_4 by a f-element-polypnictide complex. Additionally, the first systematic femtosecond (fs)-spectroscopy investigations of d/f-polypnictides are presented to showcase the advantages of having access to a broader series of lanthanide compounds.

Introduction

From the classical divalent lanthanides, Eu^{2+}, Yb^{2+}, and Sm^{2+}, which have been known since the 1920s in solution and in the solid state, Sm^{2+} has the highest redox potential and thus the broadest application as a single electron transfer (SET) reagent.[1] About two decades ago, this series was extended by the synthesis and application of the divalent iodides of Tm, Dy, and Nd.[2] Owing to the high reactivity of these compounds, their chemistry was not explored in detail, but a few divalent organometallic compounds have been prepared, e.g. $[(Cp^{ttt}_2Tm)]$ ($Cp^{ttt} = \eta^5$-1,2,4-(^{t}Bu)$_3$C$_5$H$_2$).[1b,3] Based on pioneering work by Lappert *et al.* in 1998, Evans *et al.* have established a full series of divalent rare-earth element reagents.[4] By the use of suitable reaction conditions and sterically demanding ligands it was possible to stabilize, isolate and investigate divalent molecular compounds of all lanthanides.[5] However, the synthetic potential of these new reagents has not been fully explored. While reduction of basic organic (e.g. $C_{10}H_8$, DME)[6] and inorganic compounds (e.g. N_2, CO)[1b,7] with these reagents was investigated, the access to more sophisticated compounds, such as the synthesis of Zintl compounds, is not known. Zintl ions and Zintl phases are a long known and well established class of compounds in solid-state chemistry,[8] e.g., lanthanide pnictide compounds have been discussed as potential thermoelectrical devices or solar cells.[9] In contrast to this and to molecular d-block polypnictides,[10] the molecular f-block polypnictides are still scarce and a highly promising and emerging research topic for the in-depth understanding of the reactivity and properties of this yet rarely found combination of elements. Most of the known molecular lanthanide polypnictides were synthesized by SET starting from Sm^{2+} compounds.[11] However, in terms of optical and magnetic applications, it is a strong limitation having access to Sm compounds only. In light of the availability of non-classical divalent lanthanide reagents, we felt challenged to synthesize molecular lanthanide Zintl compounds by reduction over a wider variety of 4f-elements. Here, we had to find the right balance between reactivity and stability of the corresponding lanthanide reagent, which should also offer the possibility of a subsequent coordination at resulting reduction products. As target compounds we have chosen d/f-polypnictides, which are well accessible for samarium by reacting with Sm^{2+} compounds. For this reason, e.g. $[Cp^*Fe(\eta^5\text{-}E_5)]$ (E = P, As) are suitable starting materials, for which also the reduction with K/KH was studied.[11d–f,12] By including compounds "beyond Sm"

[a] N. Reinfandt, Dr. C. Schoo, Dr. R. Yadav, Prof. Dr. P. W. Roesky
Institut für Anorganische Chemie
Karlsruher Institut für Technologie (KIT)
Engesserstr. 15, Geb. 30.45, 76131 Karlsruhe (Germany)
E-mail: roesky@kit.edu

[b] N. Michenfelder, Prof. Dr. A. N. Unterreiner
Institut für Physikalische Chemie
Karlsruher Institut für Technologie (KIT)
Fritz-Haber-Weg 2, Geb. 30.44, 76131 Karlsruhe (Germany)

[c] S. Reichl, Prof. Dr. M. Scheer
Institut für Anorganische Chemie
Universität Regensburg
Universitätsstraße 31, 93040 Regensburg (Germany)

[d] Prof. S. N. Konchenko
Nikolaev Institute of Inorganic Chemistry SB RAS
Prosp. Lavrentieva 3, 630090 Novosibirsk (Russia)

Supporting information for this article is available on the WWW under https://doi.org/10.1002/chem.202100605

we intend to get a deeper understanding of the optical properties of d/f-polypnictides.

Therefore, femtosecond (fs) transient broadband absorption spectroscopy extending from the UV to the NIR regime can be applied to obtain information about the relaxation dynamics of the pertinent electronic states of the target molecules. This is a particularly versatile method for samples, which do not show significant luminescence because other processes dominate, leading eventually to transient excited state absorption. These include charge transfer and structural rearrangement in electronically excited states. In this context, the NIR spectral region gives further information about energy transfer of lower-lying excited states, e.g. triplet states[13] or weakly bound species like contact pairs[14] or solvated electrons.[15] These are often accessible through different relaxation channels like internal conversion or intersystem crossing of inorganic compounds in solution and are strongly influenced by lanthanide complexation[16] for example in relation to spin properties. Consequently, various approaches for tuning excited state lifetimes seem feasible by ligand and lanthanide variation, requiring careful characterization in regard to energy transfer behavior.[16c]

Herein, we report on the synthesis of new d/f-polyphosphides and d/f-polyarsenides, by applying reducing agents, featuring the non-classical divalent lanthanides La, Ce, and Nd. The chemical and optical properties of the obtained compounds were further investigated by small molecule activation and fs-spectroscopy.

Results and Discussion

The divalent lanthanum compound [K(18-crown-6)(thf)$_2$][(Cp''$_2$La)$_2$(μ-η^6:η^6-C_6H_6)] (**A**) (Cp'' = $C_5H_3(SiMe_3)_2$) was first reported in 1998 by Lappert *et al.* but was crystallographically characterized by Evans *et al.* only recently.[4a,6b] This compound features two divalent lanthanum atoms, bridged by a planar $(C_6H_6)^-$ anion and imparts an exceptional thermal stability up to 70 °C (Scheme 1).[4a,6b] It can also serve as formally multi-electron reducing agent.[6b] Therefore, **A** seems to be a suitable starting point to explore the reductive synthesis of d/f-polypnictides with non-classical divalent lanthanide compounds. **A** was prepared according to the literature (Scheme 1)[4a] and reacted with [Cp*Fe(η^5-P_5)], resulting in the formation of an anionic La/Fe-polyphosphide complex [K(18-crown-6)][Cp''$_2$La(μ-η^4:η^4-P_5)FeCp*] (**1**) (Scheme 2). Recrystallization from hot toluene yielded dark-greenish crystals of **1** in moderate 30% yield. In general, all yields reported in this contribution are based on crystalline material for an unequivocal determination of the composition. Complex **1** features a monoanionic d/f-polyphosphide with a [K(18-crown-6)]$^+$ counter cation (Figure 1). To the best of our knowledge, **1** represents the first d/f-polypnictide derived from the reduction of a transition metal complex with a non-classical divalent lanthanide compound. Owing to the moderate yield and no isolable side product(s), the exact reaction pathway cannot be deduced.

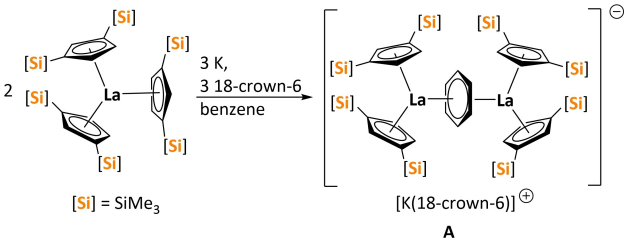

Scheme 1. Synthesis of [K(18-crown-6)][(Cp''$_2$La)$_2$(μ-η^6:η^6-C_6H_6)] (**A**) according to Lappert *et al.*[4a]

However, upon reaction, [Cp*Fe(η^5-P_5)] is reduced twice, resulting in a [Cp*Fe(η^4-P_5)]$^{2-}$ anion with an envelope shaped *cyclo*-P_5 ring. While the P_4 unit is nearly planar (torsion angle P2–P3–P4–P5: 0.95°), P1 deviates from this plane with an angle of 51.2°. As observed in similar compounds, one negative charge is localized on the phosphorus atom, which is out of plane, while the remaining negative charges are delocalized over the P_4-plane.[12a] The P–P bond distances range between 2.1580(10) Å (P3–P4) and 2.2141(9) Å (P4–P5) and are slightly longer for P2–P3/P4–P5 compared to the other three bonds. By coordinating in a η^4-coordination mode to the *cyclo*-P_5 unit, the iron atom still obeys the 18 valence-electron rule. In contrast to the reduction of [Cp*Fe(η^5-P_5)] with the classical SET agents [Cp*$_2$Sm(thf)$_2$] or [(DippForm)$_2$Sm(thf)$_2$] (DippForm = {(2,6-^{i}Pr$_2$C$_6$H$_3$)NC(H) = N(2,6-^{i}Pr$_2$C$_6$H$_3$)}$^-$) a dimerization of the P_5 unit towards P_{10} or a THF ring opening reaction is not observed here. Obviously, due to the use of a multi electron reducing agent **A**, the second reduction step ([Cp*Fe(η^4-P_5)]$^-$ to [Cp*Fe-

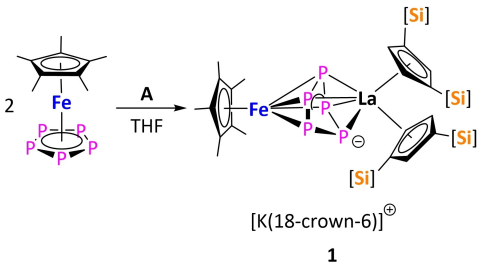

Scheme 2. Synthesis of **1**.

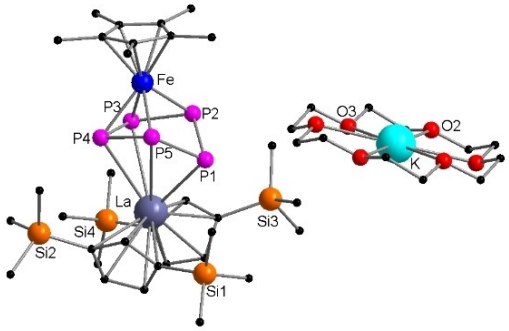

Figure 1. Molecular structure of **1** in the solid state. Solvent molecules and hydrogen atoms are omitted for clarity. For bond lengths and angles see Supporting Information (Figure S26).

(η^4-P_5)]$^{2-}$) is preferred over a radical dimerization ([Cp*Fe(η^4-P_5)]$^-$ to [(Cp*Fe)$_2$(μ,η^4-P_{10})]$^-$) or THF activation.[11e,17] For charge balance a trivalent [LaCp''$_2$]$^+$ unit coordinates in a η^4-mode to the P_5^{3-} unit, resulting in the formation of an anionic d/f-polyphosphide. Due to steric restrictions and the charge distribution, the La atom coordinates asymmetrically resulting in La–P bond distances, which range from 2.8714(6) Å (La–P1) to 3.4457(6) Å (La–P5). While the two medium La–P interaction are in the range of known La–P bond lengths reported in literature,[11i] the longest bond indicates a much weaker interaction of La–P5 (3.4457(6) Å). In contrast, the La–P1 bond (2.8714(6) Å) is significantly shortened owing to the localized charge on the protruding phosphorus atom.[12a]

The ^{1}H NMR spectrum of **1** shows two singlets, separated by 0.2 ppm, for the trimethylsilyl groups. This indicates a hindered rotation of the corresponding rings in solution. As a result, also 5 different signals are observed for the carbon atoms in the Cp''

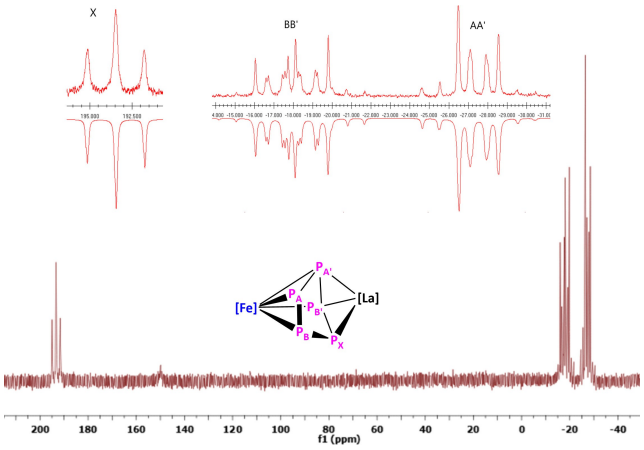

Figure 2. ^{31}P-NMR spectrum (162.0 MHz, 298 K, thf-d_8) of compound **1** with nuclei assigned to an AA'BB'X spin system; insets: extended signals (upwards) and simulations (downwards); [Fe] = [FeCp*], [La] = [LaCp''$_2$]$^+$.

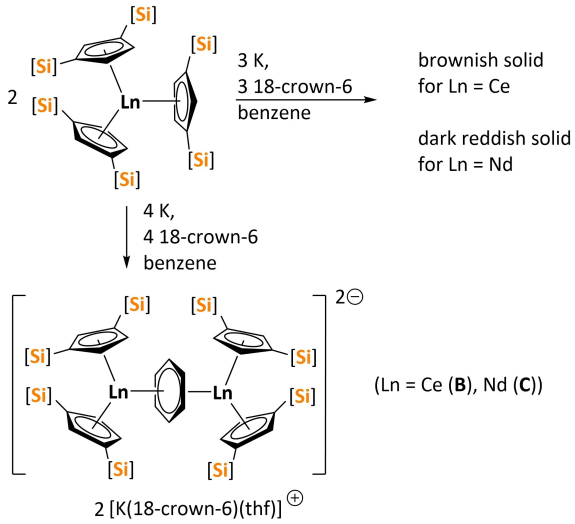

Scheme 3. Investigated reductions of [CeCp'''$_3$] and [NdCp'''$_3$] (analogous towards the synthesis of **A**) and synthesis of **B** (Ln = Ce) and **C** (Ln = Nd).

ring in the ^{13}C{^{1}H} NMR spectrum. The ^{31}P{^{1}H} NMR spectrum of **1** shows an AA'BB'X spin system with three sets of multiplets at δ −27, −18 and 193 ppm (Figure 2). Such an AA'BB'X spin system is typical for a reduced cyclic P_5 unit.[12a] By iterative simulation, the multiplet at 193 ppm can be assigned to the out of the plane phosphorus P_X, the multiplet at −18 ppm to $P_{B,B'}$ and the one at −27 ppm to $P_{A,A'}$.

After the successful synthesis of **1**, we were intrigued whether an analogous reaction would be possible for other non-classical divalent lanthanides. Therefore, we investigated the synthesis of the Ce and Nd analogs of **A** (Scheme 3). The reaction of [LnCp''$_3$] (Ln = Ce, Nd) in benzene with 1.5 equivalents of potassium at room temperature (starting at −78 °C, slowly warming to room temperature) for seven days yielded a dark brownish (Ce) or purple-reddish (Nd) solid. For Ce, only low quality crystals were obtained. Although, we could not determine its structure by single crystal X-ray diffraction, NMR studies and further reactivity indicates the existence of a species analogous to **A** (see Figure S13). In contrast, the crystallization (THF/Et$_2$O at −35 °C) of the raw product from the reduction of the Nd precursor showed the formation of the unexpected compound [K(18-crown-6)(thf)]$_2$[(Cp''$_2$Nd)$_2$(μ-η^6:η^6-C_6H_6)] (**C**, Scheme 3). In contrast to **A**, compound **C** features a [(Cp''$_2$Nd)$_2$(μ-η^6:η^6-C_6H_6)]$^{2-}$ dianion, which formally may act as a 4-electron reducing agent.

The lower reduction potential of Nd compared to La and Ce (−2.6 vs −3.1/−3.2 V vs. NHE)[18] seems to favor the additional reduction step, resulting directly in the 4-fold reduced species **C**.

After these initial results, we optimized the reaction conditions. By using two equivalents of potassium and 18-crown-6 the formally 4-fold reduced compounds [K(18-crown-6)(thf)]$_2$[(Cp''$_2$Ln)$_2$(μ-η^6:η^6-C_6H_6)] (Ln = Ce (**B**), Nd (**C**), Scheme 3) were obtained in a rational manner and with improved yields as dark purple crystals.

Compounds **B** (Figure S24) and **C** (Figure 3) crystallize in the orthorhombic space group *Fddd* with 0.25 molecules in the asymmetric unit. In contrast to **A**, the {LnCp''$_2$} moieties have a

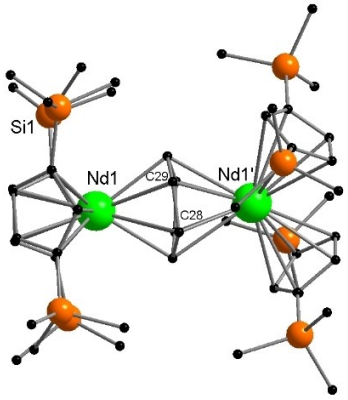

Figure 3. Molecular structure of **C** in the solid state. Solvent molecules, counter-cations and hydrogen atoms are omitted for clarity. For bond lengths and angles see Supporting Information (Figure S25). For compound **B** see Figure S24.

staggered and not an ecliptic conformation.[6b] While free benzene has an average bond length of 1.397(9) Å,[19] the C–C bonds in the C_6-unit (1.442(5)–1.455(8) Å) are longer. The non-planar C_6-moiety has a dihedral angle of ~14.8°. Comparison of these values with the just recently reported similar 4-electron reducing agent [K(2.2.2-cryptand)]$_2$[(Cp′$_2$La)$_2$(μ-η^6:η^6-C_6H_6)] and a reported $(C_6H_6)^{4-}$ -unit, which is planar and has even longer C–C-bonds (average of 1.47 Å), strongly supports the existence of a $(C_6H_6)^{2-}$ -unit.[20] Nevertheless, the slightly smaller dihedral angle in [K(2.2.2-cryptand)]$_2$[(Cp′$_2$La)$_2$(μ-η^6:η^6-C_6H_6)] (11° in comparison to 12.8° (**B**) and 14.8° (**C**)) indicates an influence of the additional trimethylsilyl-groups and the different lanthanides upon the electronic structure of the compound.[20a] The distance from Nd towards the centroids of the Cp ligands is 2.64 Å and therefore 0.12 Å longer than in [NdCp′′$_3$],[21] which is expected for Nd(II) compounds. The benzene ring is tilted along the Nd–Nd′ axis. Therefore, a short Nd–$C_{benzene}$ bond corresponds with a long Nd′–$C_{benzene}$ distance, e.g. Nd1′–C28 2.738(4) Å, Nd1–C28 2.559(4) Å.

An analogous synthetic approach for the corresponding La compound was not successful. Our observation, that the selective formation of low valent lanthanide compounds depends on the lanthanide, the reaction conditions (stoichiometric ratio, time, temperature, potassium chunks vs. potassium mirror or KC_8), the ligand, and the counter ion, matches with earlier work on the reduction of [LnCp′′$_3$] (Ln = La, Ce, Pr, Nd).[4a,7,20a,22]

After the synthesis of two new lanthanide based, non-classical 4-electron reducing reagents **B** and **C**, we were intrigued to study their reactivity and to compare it with **A**. The reaction of **B** and **C** with [Cp*Fe(η^5-P_5)] resulted in the formation of the complex salts [K(18-crown-6)][Cp′′$_2$Ce(μ-η^4:η^4-P_5)FeCp*] (**2**) and [K(18-crown-6)][Cp′′$_2$Nd(μ-η^4:η^4-P_5)FeCp*] (**3**) (Scheme 4). Therefore, the reaction product is not affected by applying **B** or **C** instead of **A**. However, the use of a four electron reducing agent allowed the reduction process to proceed in a stoichiometric ratio and hence, resulted in better yields for complex **2** (53%) and **3** (59%) than for the synthesis of **1** (30%). The use of the raw product of the expected 3-electron reducing agent of Ce (see above) resulted also in compound **2** but with a lower yield (ca. 30%, comparable to **1**). In the solid-state, complex **2** and **3** are similar to **1** but the relative orientation of the counter cation differs (Figure 4). Again, a [Cp*Fe(η^4-P_5)]$^{2-}$ anion with an

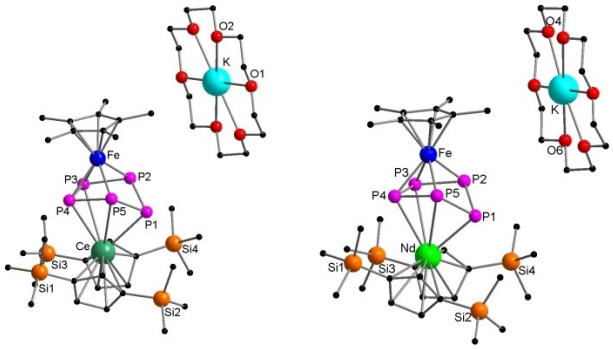

Figure 4. Molecular structures of **2** (left) and **3** (right) in the solid state. Solvent molecules and hydrogen atoms are omitted for clarity. For bond lengths and angles see Supporting Information (Figures S27 and S28).

envelope shaped *cyclo*-P_5 ring is formed. For all three compounds the P4–P5 bond is the longest phosphorus bond. Due to the smaller ionic radius, the Ln–P distances are decreasing from La to Ce and Nd (Ln–P1 (Ln = La, Ce, Nd): 2.8714(6) Å, 2.854(2) Å, 2.8317(11) Å). All other bond parameters are comparable to **1**. To the best of our knowledge, complex **2** and **3** represent the first examples of Ce- and Nd–polyphosphide complexes.

After the successful synthesis of these three new d/f-polyphosphides, we were interested whether this approach is applicable to the reduction of the corresponding d-metal polyarsenide [Cp*Fe(η^5-As_5)].

In general, the reactivity of d-metal polyarsenides is significantly less investigated compared to the d-metal polyphosphides. [Cp*Fe(η^5-As_5)] was reduced with the 3- and 4-electron reducing agents **A**, **B** and **C**. By using a reaction protocol similar to the synthesis of **1**, **2** and **3** and subsequent recrystallization from hot toluene, the new d/f-polyarsenide complex salts [K(18-crown-6)][Cp′′$_2$Ln(μ-η^4:η^4-As_5)FeCp*] (Ln = La (**4**), Ce (**5**) and Nd (**6**)) were obtained (Scheme 5, Figure 5) in moderate yield. To the best of our knowledge, compounds **4**–**6** are the first molecular polyarsenides of the corresponding elements.

Analogous to the synthesis of **1**–**3**, the yields are higher while using the 4-electron reducing agents **B** and **C** (20% for **A** vs. 40% for **B** and **C**). All three compounds are isostructural to each other (Figure 5). Hence, only compound **4** is discussed in

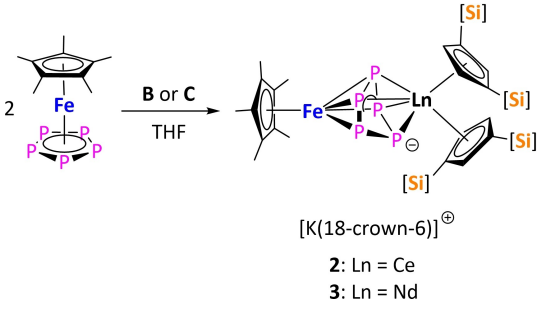

Scheme 4. Synthesis of **2** (Ln = Ce) and **3** (Ln = Nd).

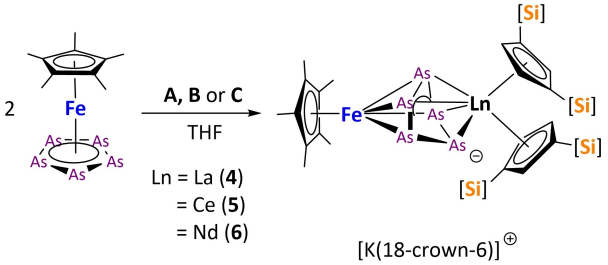

Scheme 5. Synthesis of the d/f-polyarsenide complex salts **4** (Ln = La), **5** (Ln = Ce) and **6** (Ln = Nd).

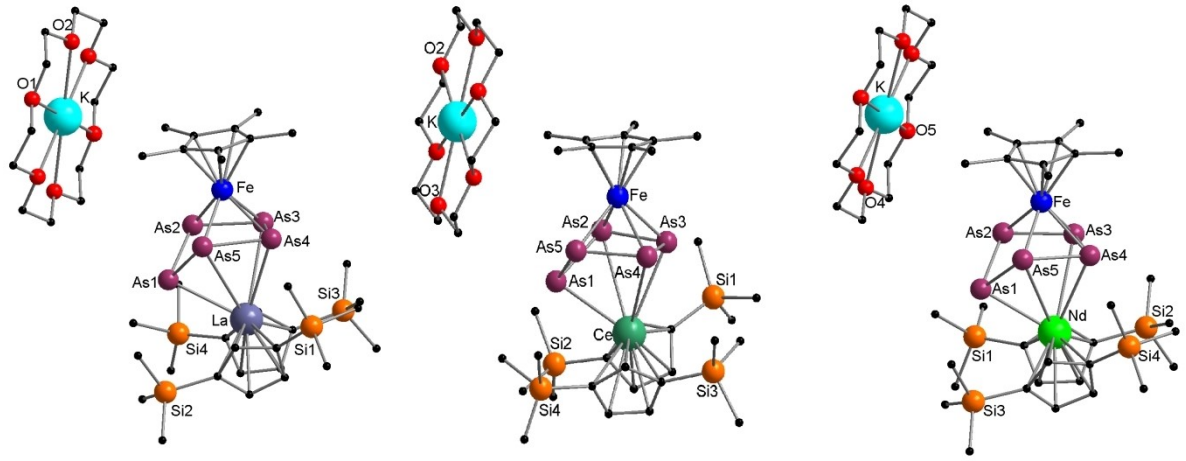

Figure 5. Molecular structures of **4** (left), **5** (middle) and **6** (right) in the solid state. Solvent molecules and hydrogen atoms are omitted for clarity. For bond lengths and angles see Supporting Information (Figures S29–S31).

detail. Analogous to the reduction of [Cp*Fe(η^5-P_5)], [Cp*Fe(η^5-As_5)] is reduced twice, resulting in a [Cp*Fe(η^4-As_5)]$^{2-}$ anion with an envelope shaped *cyclo*-As_5 ring. While the torsion angle of the As_4 unit is smaller as in **1** (torsion angle As2–As3–As4–As5: 0.36° vs. 0.95°), the deviation of As1 from this plane is slightly larger (53.3° vs. 51.2°). As seen for the analogous phosphorus compounds, the iron atom is η^4-coordinated to the *cyclo*-As_5 unit. The shortest As–As bond distance is observed between As3–As4 (2.3781(6) Å), while the other bonds range from 2.3928(5) Å to 2.4325(5) Å, which compares well with other known As–As-bonds.[12b,17] Due to steric constraints and charge distribution, the Ln–As bond lengths vary over a wide range. Thus, the Ln–As bond length is significantly shortened in comparison to the other three bonds (La–As1 2.9631(4) Å, La–As3 3.4453(4) Å, La–As4 3.1922(4) Å, La–As5 3.5330(5) Å). While the influence of the lanthanide contraction is less distinct for the Ln–As1 bonds as for the Ln–P bonds in **1**–**3**, it is observed for the Ln–As5 bonds (Ln = La 3.5330(5) Å, Ce 3.5075(8) Å, Nd 3.4669(5) Å). This indicates an influence of steric and packing effects upon coordination of the [LnCp''$_2$]$^+$ moiety at the [Cp*Fe(η^4-As_5)]$^{2-}$ unit. The ^{1}H NMR-spectrum of **4** is comparable to **1**, indicating a restricted rotation of the Cp''-rings. The clean isolation of **4**–**6** is quite remarkable, because the reduction of [Cp*Fe(η^5-As_5)] with other reducing agents such as KH or [Cp$^{tt}_2$Sm(thf)] resulted either in a mixture of products, compounds without an intact As_5 unit or some subsequent reactivity.[11f,12b,17]

After the synthesis of the series of six new d/f-polypnictides we studied their further reactivity and the influence of the coordinated lanthanide moiety. To the best of our knowledge, no specific reactivity studies of any lanthanide polypnictides are reported. After reducing the E_5-ring (E = P, As) in [Cp*Fe(η^5-E_5)], we aimed for an expansion of the E_5-unit. Analogous to the reactivity of [K]$_2$[Cp*Fe(η^4-P_5)],[12a] we chose the activation of P_4 as model reaction.

Reaction of **1** and **3** with half an equivalent of P_4 at room temperature resulted in a clear, green-reddish solution (Scheme 6). Crystals of the corresponding reaction products [K(18-crown-6)][Cp''$_2$Ln(P_7)FeCp*] (Ln = La (**7**), Nd (**8**)), featuring a P_7^{3-} unit, were obtained by slow evaporation of a saturated THF (**7**) or toluene (**8**) solution. Upon activation and break-up of a P_4 molecule, a P_2 unit inserts selectively into the [Cp*FeP_5]$^{2-}$ moiety to form a [Cp*FeP_7]$^{2-}$ anion with a typical norbornadiene structure of the P_7 moiety (Figure 7). The observed selective expansion of the P_5-unit is, to the best of our knowledge, the first example of a P_4 activation by f-polypnictide complexes. According to NMR-experiments, the reaction proceeds in a quantitative manner. Overall, it is remarkable that the coordination of a stabilizing and sterically demanding lanthanide moiety to the polyphosphide does not significantly reduce the reactivity of highly charged polyphosphides in coordinating or non-coordinating solvents. Therefore, compounds of the type of **1**–**3** are promising candidates for further reactivity studies of highly charged polypnictides, featuring a much better stability and solubility as for example [K]$_2$[Cp*Fe(η^4-P_5)].[12a] Compound **7** shows the expected ^{1}H NMR spectra in toluene-d_8. The influence of the P_7^{3-} moiety upon the electronic structure of the compound can best be seen by the signal for the Cp* ligand, which is shifted from 1.31 ppm in **1** to 1.61 ppm in **7**. Interestingly, **7** shows a dynamic behavior upon dissolving in the coordinating solvent thf-d_8. By VT-NMR measurements, it is possible to obtain ^{31}P{^{1}H} NMR spectra, which are suitable for the simulation (Figure 6, for details see Supporting Information).

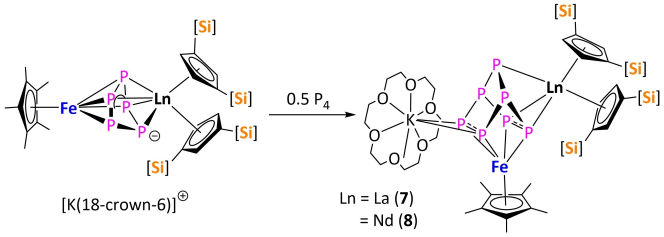

Scheme 6. Synthesis of **7** (Ln = La) and **8** (Ln = Nd) by activation of P_4.

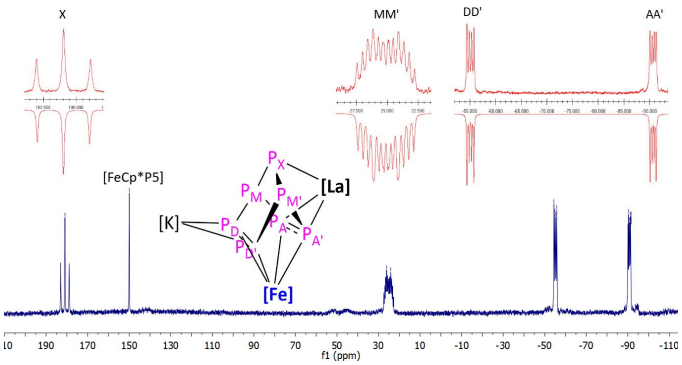

Figure 6. ^{31}P NMR spectrum (162.0 MHz, 253 K, thf-d_8) of compound **7** with nuclei assigned to an AA'DD'MM'X spin system; insets: extended signals (upwards) and simulations (downwards); [Fe] = FeCp*, [La] = $[LaCp''_2]^+$, [K] = $[K(18\text{-crown-6})]^+$.

By iterative simulation, the multiplet at 182 ppm can be assigned to the phosphorus P_X, the multiplet at 25 ppm to $P_{MM'}$, the one at −55 ppm to $P_{D,D'}$ and the one at −90 to $P_{A,A'}$. While the multiplets at −55 and −90 ppm become better resolved at lower temperatures, it is vice versa for the multiplet at 25 ppm (Figure S10–11). This indicates at least two different dynamic behaviors in solution (e.g. tumbling of the Ln bonds or the K atoms).

It is seen from the solid-state structure of **7** and **8** (Figure 7), that P1 and P3 deviate from the P4–P5–P6–P7-plane with an angle of 72° (P1) and 70° (P3). This is around 20° larger than in **1**–**3**. The P–P bonds are comparable to similar compounds in the literature.[23] While the P–P bond lengths from P1 and P3 to the P4–P5–P6–P7 plane are in the range of single bonds (2.221(2) Å–2.262(2) Å) the bond lengths in the plane are, due to their double bond character, slightly shorter (2.128(3) Å–2.178(4) Å). Also, the bond lengths towards the apical P2 atom is shortened (2.157(2)–2.173(2) Å), which may be explained by the delocalization of the negative charge on the latter.[23–24]

The shortest Ln–P bond lengths are seen for the two-fold bonded and charged apical P-atom (La–P2 2.979(2) Å, Nd–P2 2.914(3) Å), the second shortest towards P4 and P5 (La–P4 3.073(2) Å, La–P5 3.136(2) Å) and the longest bonds towards P1 and P3 (La–P1 3.464(2) Å, La–P3 3.436(2) Å).

After the successful activation of P_4 by the d/f-polyphosphides, and due to the fact that an analogous As_7 structure motif is known,[11f] we were intrigued to study the same reactivity for the d/f-polyarsenides aiming for mixed P/As-polypnictides. The reaction of **4**–**6** with half an equivalent of P_4 resulted in a green-orange solution. NMR scale reactions revealed a shift of the Cp* signal, comparable to the synthesis of **7** and **8**. However, ^{31}P NMR studies of the reactions at room temperature did not show any signals besides that of white phosphorus. Upon crystallization, poor quality crystals were obtained, featuring an E_7 moiety. After redissolving the latter in thf-d_8, decomposition within days resulted in several ^{31}P NMR signals, indicating indeed the existence of a mixed polypnictide. Therefore, the before mentioned missing signals in the ^{31}P NMR measurements at room temperature hint at a highly fluctuating behavior of the possibly incorporated P atoms at room temperature. However, owing to the bad solubility in toluene and the low stability of the compounds in THF, VT NMR-measurements could not elucidate further details on the composition of the E_7 moiety.

The newly synthesized d/f-polyphosphides **1**–**3** and d/f-polyarsenides **4**–**6** were studied in terms of their electronic properties. To the best of our knowledge, no ultrafast time resolved studies were reported on *cyclo*-P_5 and *cyclo*-As_5 complex dynamics. Therefore, we investigated the influence of different Ln atoms bound to *cyclo*-P_5 and *cyclo*-As_5 rings, respectively, with special view on reference systems without lanthanide substitution. This approach will also allow for elucidation of the influence of P and As rings as ligand systems. In Figure 8, the stationary absorption spectra of complexes **1**–**3** and **4**–**6** and the respective [Cp*Fe(η^5-E_5)] compounds in THF solution are shown. For all phosphide complexes (**1**–**3**), broad UV absorption bands with comparable shoulders and an additional band peaking at 590 nm are seen; they are also similar to the reference system [Cp*Fe(η^5-P_5)] except for some additional features in the UV range. For [Cp*Fe(η^5-As_5)], absorption bands show a red shift compared to the P analogue, but the overall band shape is broadly maintained in line with

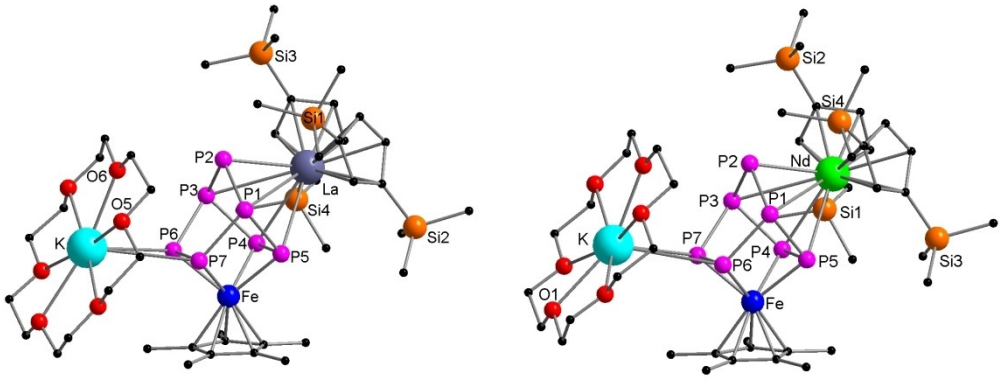

Figure 7. Molecular structure of **7** (left) and **8** (right) in the solid state. Solvent molecules and hydrogen atoms are omitted for clarity. For bond lengths and angles see Supporting Information (Figures S32 and S33).

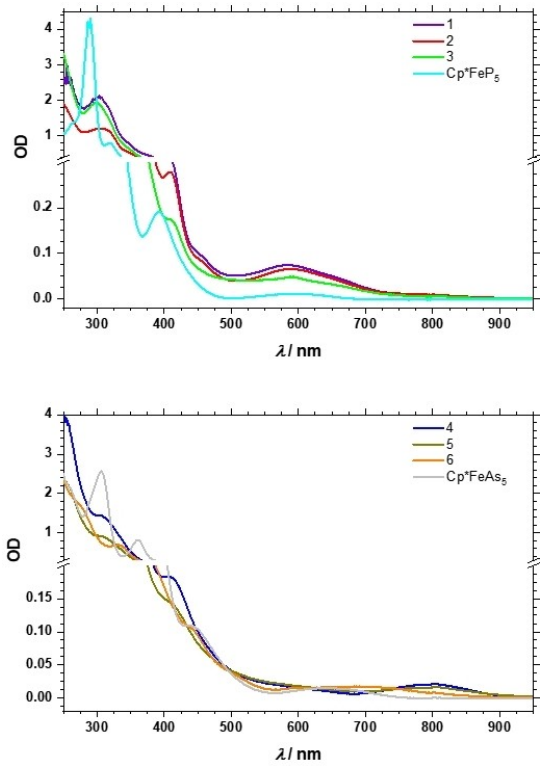

Figure 8. Stationary absorption spectra of the P_5 complexes (**1**–**3**) top and the As_5 complexes (**4**–**6**) bottom in THF solution. The respective [Cp*Fe(η^5-E_5)] is also shown for comparison.

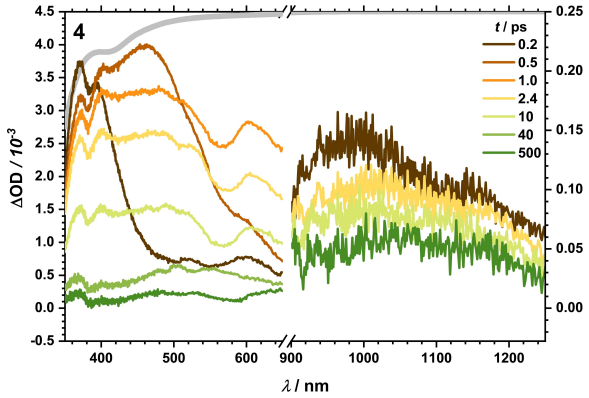

Figure 9. Raw data transient absorption spectra at given delay times after 267/258 nm excitation for **4**. The differing pump for UV/Vis (267 nm) and NIR (258 nm) are due to different laser systems used for the experiments. For more information, see the Methods section and Supporting Information. Note the different ΔOD scale for UV/Vis (left axis) and NIR (right axis) probe. For further details, see main text.

previous investigations of *cyclo*-P_5 and *cyclo*-As_5 rings.[25] The red-shifted *cyclo*-As_5 complexes (**4**–**6**) exhibit further red-shifts depending on the lanthanide. For example, the absorption band around 650 nm of [Cp*Fe(η^5-As_5)] exhibits a small shift of 30 nm (0.08 eV) for the Nd complex **6**, whereby **4** and **5** show a larger shift of 150 nm (0.35 eV). Independent of the ring system, the UV bands can be attributed to LMCT (LMCT = ligand to metal charge transfer) of the lanthanide entity, d–f-[6a,16c,26] and ππ* transitions of the P_5 ring around 264 and 320 nm[25] as well as Fe–Cp LMCT (320–330 nm).[27] The low energy band of all compounds may be attributed to a CT (CT = charge transfer, vide infra). Comparing As and P, the influence of the lanthanide seems to be much more relevant for the As-compounds. In all cases, fluorescence was not observed, which is typical for low-lying LMCT transitions.[28]

As an example of the transient absorption spectra after 267/258 nm excitation, we first concentrate on compound **4** (Figure 9). In the Vis and NIR regions, broad absorption bands peaking between 400–500 nm can be observed. After correction of the group velocity mismatch of pump and probe pulses, transient traces for all investigated probe wavelengths show an immediate rise at $t = 0$ ps (see Figure S34, left). For further data evaluation, the transient response was fitted globally with three exponential decays (for a more detailed description see Supporting Information). The resulting fit curves are depicted in Figure S34. After the pump-induced rise, a first component with $\tau_1 = 200$ fs is followed by a slower decay of $\tau_2 = 8.3$ ps (ps = picoseconds). In the NIR range, an additional decay on a longer time scale ($\tau_3 \sim 500$ ps) is much more pronounced than in the UV/Vis range. Owing to the limited maximum range of the delay stage of roughly 1.2 ns, τ_3 can only be considered as a rough assessment. Transient spectra of **1**, **2**, **3**, **5** and **6** look similar to **4** (see Supporting Information Figures S34) and the resulting time constants of all compounds are shown in Table 1. To describe the relaxation dynamics of the d/f-polypnictides, we adapt a mechanism successfully applied for bulk materials like α-Fe_2O_3 nanoparticles,[29] colloidal solutions,[30] thin films,[31] and on a molecular level for methyl-triethanolamine ligated $Fe_{10}Ln_{10}$ coordination clusters[16c] as well as [Ge_9(Hyp)$_3$FeCp(CO)$_2$][32] (Hyp = $Si(SiMe_3)_3$) clusters. After UV excitation into an excited quasi-continuum (high density of states), the deactivation process partitions into three different steps as illustrated in Figure 10. The first step at a timescale of $\tau_1 = 200$ fs comprises various relaxation processes in the excited electronic state, which are not distinguishable from transient absorption spectra alone, inter alia vibrational relaxation (VR) including vibrational redistribution and charge localization within the excited quasi-continuum in competition to trapping into long-lived individual states. The second step is geminate recombination of those population being localized in charge transfer states. Typical lifetimes are on the ps timescale[33] which fits our second time constant ($\tau_2 = 4$–8 ps).

Table 1. Time constants from global fitting after 267/258 nm excitation.

	1	**2**	**3**	[Cp*FeP_5]
τ_1/ps	0.2	0.4	0.5	0.3
τ_2/ps	7.1	6.3	5.2	4.5
τ_3/ps	~500	~1000	~800	~200
	4	**5**	**6**	[Cp*$FeAs_5$]
τ_1/ps	0.2	0.5	0.3	0.3
τ_2/ps	8.3	6.3	4.3	5.0
τ_3/ps	~500	~1000	~1000	~200

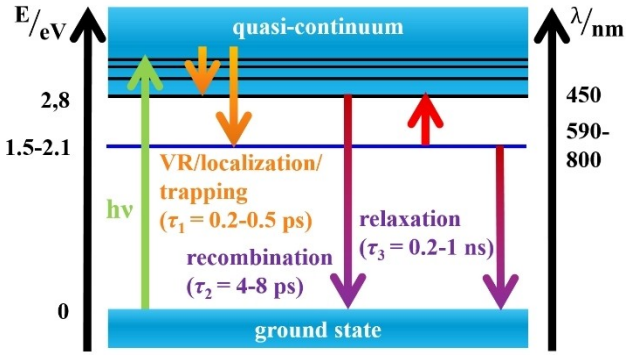

Figure 10. Sketch showing possible relaxation pathways. The band model serves as simplification. Green arrow: excitation; orange arrows: VR, localization and trapping; violet arrows: recombination and relaxation back into the ground state; red arrow: absorption of the trap states. For further details, see text.

The third step is independent on the second one and represents ground state recovery from trapped population within some hundreds of ps ($\tau_3 = 0.2$–1 ns) or beyond. An example of trap states may be triplet states[34] or low lying, long-lived charge transfer states. On the other hand, charge transfer to $[K(18\text{-crown-6})]^+$ or the solvent is unlikely, as the long lived NIR spectral response does not match the known spectra of the K^+-electron contact pair[35] or the solvated electron[36] in THF solution.

For further analysis, the reference substances [Cp*Fe(η^5-P_5)] and [Cp*Fe(η^5-As_5)] were measured in THF solution under the same experimental conditions (see Supporting Information Figure S34). Comparing the amplitudes $A_{1,rel.}$ of **4** and [Cp*Fe(η^5-As_5)] (Table S7, Figure S35), the corresponding population in the excited state decays much stronger for [Cp*Fe(η^5-As_5)]. The influence of the lanthanide complexation on $A_{1,rel.}$ was seen for all compounds **1**–**6** in comparison to the chemical precursors. The next step of analysis is the comparison between P- and As-complexes. In Figure S36, the transient response of the Ce analogues **2** and **5** at 1200 nm and 450 nm (inset) probe wavelengths shows that the first two processes in the visible range on a sub ps and ps timescale have similar amplitudes whereas these amplitudes differ strongly in the NIR spectral range. This can also be observed by comparing the relative amplitudes in Table S7 where $A_{3,rel.}$ for compound **5** is only 20% of $A_{3,rel.}$ for the P analogue. For the other compounds, this is also observable but to a lesser extent.

The absorption spectra related to localization and back charge transfer have a defined low energy band edge, which is red shifted for the As species and therefore more pronounced in the NIR spectral range than for the P species in agreement with the trend in the stationary absorption spectra. Hence, the excited states of the As_5 species seem to be located energetically lower compared to P_5. The trap states are less influenced.

Finally, we address the influence of the different lanthanides on the excited state dynamics as, e.g. in lanthanide-based polymeric chains, a dependence of the time constants was found.[16b] At first glance, the second time constant τ_2 (see Table 1 and Figure S37) correlates with the atomic number of the lanthanide. The shortest values correspond to those for the reactants and the Nd species around 5 ps. The Ce and especially the La complexes show longer lifetimes. Hence, the influence of the lanthanides resembles a similar trend compared to the third ionization potentials[37] or electronegativities,[38] which are lowest for La and higher for Ce and Nd. For the bulk-like materials, the chromophoric entity can be attributed to an Fe–O unit where photoexcitation leads to a charge transfer from oxygen to iron.[29b] The influence of electron withdrawing effects from the Ln should be strongest for a charge transfer from the E_5-ring to the Fe atom, which supports localization within τ_1 among this charge transfer state after UV-excitation, which by itself has a lifetime τ_2. The trap state lifetime also depends on the lanthanide being longest for Nd and shortest for La. Consequently, the higher electron withdrawing effect of Nd stabilizes the trap state. The transient absorption in the NIR region can be attributed to a transition from the low-lying states, which appear between 590 and 800 nm in the stationary absorption spectrum, into the quasi-continuum (red arrow in Figure 10). Therefore, the trap states are ascribable to these low-lying charge transfer states. The effect of the lanthanide complexation clearly results in a change of the energy surfaces, which depends on the electronegativity of the lanthanides.

Conclusion

In summary, we have synthesized two new non-classical, divalent Ce (**B**) and Nd (**C**) compounds, which are formally 4-electron reducing agents and reveal a deeper understanding of the behavior of reaction mixtures containing highly reactive non-classical divalent lanthanides upon small changes. By using these reagents together with the established La compound **A**, a 3-electron reducing agent, the reduction of sophisticated organometallic compounds could be extended far beyond the established SET induced by divalent samarium. Compounds **A**–**C** were employed for the reductive synthesis of a series of new d/f-polypnictides (**1**–**6**).

The reactivity of the polyphosphides was further studied with P_4. In a redox neutral process, two P-atoms were selectively inserted into the P_5^{3-} units of **1**–**3**. The resulting complexes **7** and **8** are the first examples of a P_4 activation by f-polypnictide complexes and they are also the first isolated products derived from reactivity studies of f-element polypnictides in general. The resulting norbonadiene type P_7^{3-} moiety shows a dynamic behavior in THF solution. Due to the variety of lanthanide elements in **1**–**6**, the influence of the metal atom onto the electronic properties could be studied. Despite the isostructurality of the compounds and only minor differences in the solid state, fs-spectroscopic investigations of **1**–**6** revealed effects on the electronic structure of the d/f-polypnictides upon the use of different pnictides and lanthanides. The received deeper understanding of the electronic structure of this class of compounds is an important step towards the fine tuning of the properties of such d/f-polypnictides in the future.

Therefore, this work opens new avenues for the redox chemistry of non-classical divalent lanthanides in general. The employment of a larger variety of lanthanide elements in the redox chemistry of organometallic compounds offers the access to many potentially interesting molecules for optical and magnetic studies.

Experimental Section

Crystallographic data: Deposition numbers "2048766, 2048767, 2048768, 2048769, 2048770, 2048771, 2048772, 2048773, 2048774, and 2048775" contain the supplementary crystallographic data for this paper. These data are provided free of charge by the joint Cambridge Crystallographic Data Centre and Fachinformationszentrum Karlsruhe "Access Structures service".

Acknowledgements

We are grateful to the Deutsche Forschungsgemeinschaft (DFG) (No. 266153560, Ro 2008/17-2 and Sche 384/33-2 as well as UN108/6-1) and to the Russian Foundation for Basic Research (RFBR, grant 19-03-00568) for financial support. N.R.'s Ph.D. study is additionally funded by the Fonds der Chemischen Industrie (102431). The DFG funded Research Training Group (RTG) 2039 (Molecular architecture for fluorescent cell imaging) is acknowledged for financial support. Open access funding enabled and organized by Projekt DEAL.

Conflict of Interest

The authors declare no conflict of interest.

Keywords: femtosecond spectroscopy · lanthanides · P_4 activation · polypnictides · reduction

[1] a) W. J. Evans, *Coord. Chem. Rev.* **2000**, *206–207*, 263–283; b) F. Nief, *Dalton Trans.* **2010**, *39*, 6589–6598.
[2] a) M. N. Bochkarev, I. L. Fedushkin, A. A. Fagin, T. V. Petrovskaya, J. W. Ziller, R. N. R. Broomhall-Dillard, W. J. Evans, *Angew. Chem. Int. Ed. Engl.* **1997**, *36*, 133–135; *Angew. Chem.* **1997**, *109*, 123–124; *Angew. Chem. Int. Ed.* **1997**, *36*, 133–135; b) M. N. Bochkarev, I. L. Fedushkin, S. Dechert, A. A. Fagin, H. Schumann, *Angew. Chem. Int. Ed.* **2001**, *40*, 3176–3178; *Angew. Chem.* **2001**, *113*, 3268–3270; c) W. J. Evans, N. T. Allen, J. W. Ziller, *J. Am. Chem. Soc.* **2000**, *122*, 11749–11750.
[3] F. Jaroschik, F. Nief, L. Ricard, *Chem. Commun.* **2006**, 426–428.
[4] a) M. C. Cassani, D. J. Duncalf, M. F. Lappert, *J. Am. Chem. Soc.* **1998**, *120*, 12958–12959; b) M. R. MacDonald, J. E. Bates, J. W. Ziller, F. Furche, W. J. Evans, *J. Am. Chem. Soc.* **2013**, *135*, 9857–9868.
[5] W. J. Evans, *Organometallics* **2016**, *35*, 3088–3100.
[6] a) C. T. Palumbo, L. E. Darago, C. J. Windorff, J. W. Ziller, W. J. Evans, *Organometallics* **2018**, *37*, 900–905; b) C. T. Palumbo, L. E. Darago, M. T. Dumas, J. W. Ziller, J. R. Long, W. J. Evans, *Organometallics* **2018**, *37*, 3322–3331; c) C. M. Kotyk, M. R. MacDonald, J. W. Ziller, W. J. Evans, *Organometallics* **2015**, *34*, 2287–2295.
[7] A. J. Ryan, J. W. Ziller, W. J. Evans, *Chem. Sci.* **2020**, *11*, 2006–2014.
[8] T. F. Faessler, *Struct. Bond., Vol. 140*, Ed.: M. P. Mingos, Springer Verlag, Berlin, **2011**.
[9] a) J. M. O. Zide, A. Kleiman-Shwarsctein, N. C. Strandwitz, J. D. Zimmerman, T. Steenblock-Smith, A. C. Gossard, A. Forman, A. Ivanovskaya, G. D. Stucky, *Appl. Phys. Lett.* **2006**, *88*, 162103; b) M. P. Hanson, A. C. Gossard, E. R. Brown, *Appl. Phys. Lett.* **2006**, *89*, 111908; c) W. Kim, J. Zide, A. Gossard, D. Klenov, S. Stemmer, A. Shakouri, A. Majumdar, *Phys. Rev. Lett.* **2006**, *96*, 045901.
[10] R. J. Wilson, B. Weinert, S. Dehnen, *Dalton Trans.* **2018**, *47*, 14861–14869.
[11] a) S. N. Konchenko, N. A. Pushkarevsky, M. T. Gamer, R. Köppe, H. Schnöckel, P. W. Roesky, *J. Am. Chem. Soc.* **2009**, *131*, 5740–5741; b) C. Schoo, S. Bestgen, A. Egeberg, J. Seibert, S. N. Konchenko, C. Feldmann, P. W. Roesky, *Angew. Chem. Int. Ed.* **2019**, *58*, 4386–4389; *Angew. Chem.* **2019**, *131*, 4430–4434; c) C. Schoo, S. Bestgen, A. Egeberg, S. Klementyeva, C. Feldmann, S. N. Konchenko, P. W. Roesky, *Angew. Chem. Int. Ed.* **2018**, *57*, 5912–5916; *Angew. Chem.* **2018**, *130*, 6015–6019; d) T. Li, J. Wiecko, N. A. Pushkarevsky, M. T. Gamer, R. Köppe, S. N. Konchenko, M. Scheer, P. W. Roesky, *Angew. Chem. Int. Ed.* **2011**, *50*, 9491–9495; *Angew. Chem.* **2011**, *123*, 9663–9667; e) T. Li, M. T. Gamer, M. Scheer, S. N. Konchenko, P. W. Roesky, *Chem. Commun.* **2013**, *49*, 2183–2185; f) N. Arleth, M. T. Gamer, R. Köppe, S. N. Konchenko, M. Fleischmann, M. Scheer, P. W. Roesky, *Angew. Chem. Int. Ed.* **2016**, *55*, 1557–1560; *Angew. Chem.* **2016**, *128*, 1583–1586; g) T. Li, S. Kaercher, P. W. Roesky, *Chem. Soc. Rev.* **2014**, *43*, 42–57; h) W. Huang, P. L. Diaconescu, *Chem. Commun.* **2012**, *48*, 2216–2218; i) W. Huang, P. L. Diaconescu, *Eur. J. Inorg. Chem.* **2013**, 4090–4096; j) D. Patel, F. Tuna, E. J. L. McInnes, W. Lewis, A. J. Blake, S. T. Liddle, *Angew. Chem. Int. Ed.* **2013**, *52*, 13334–13337; *Angew. Chem.* **2013**, *125*, 13576–13579.
[12] a) M. V. Butovskiy, G. Balázs, M. Bodensteiner, E. V. Peresypkina, A. V. Virovets, J. Sutter, M. Scheer, *Angew. Chem. Int. Ed.* **2013**, *52*, 2972–2976; *Angew. Chem.* **2013**, *125*, 3045–3049; b) M. Schmidt, D. Konieczny, E. V. Peresypkina, A. V. Virovets, G. Balázs, M. Bodensteiner, F. Riedlberger, H. Krauss, M. Scheer, *Angew. Chem. Int. Ed.* **2017**, *56*, 7307–7311; *Angew. Chem.* **2017**, *129*, 7413–7417.
[13] C. Bräuchle, U. P. Wild, D. M. Burland, G. C. Bjorklund, D. C. Alvarez, *Opt. Lett.* **1982**, *7*, 177–179.
[14] B. Bockrath, L. M. Dorfman, *J. Phys. Chem.* **1973**, *77*, 1002–1006.
[15] L. M. Dorfman, F. Y. Jou, R. Wageman, *Ber. Bunsen-Ges.* **1971**, *75*, 681–685.
[16] a) H. Rothfuss, N. D. Knöfel, P. Tzvetkova, N. C. Michenfelder, S. Baraban, A.-N. Unterreiner, P. W. Roesky, C. Barner-Kowollik, *Chem. Eur. J.* **2018**, *24*, 17475–17486; b) D. T. Thielemann, M. Klinger, T. J. A. Wolf, Y. Lan, W. Wernsdorfer, M. Busse, P. W. Roesky, A.-N. Unterreiner, A. K. Powell, P. C. Junk, G. B. Deacon, *Inorg. Chem.* **2011**, *50*, 11990–12000; c) A. Baniodeh, Y. Liang, C. E. Anson, N. Magnani, A. K. Powell, A.-N. Unterreiner, S. Seyfferle, M. Slota, M. Dressel, L. Bogani, K. Goß, *Adv. Funct. Mater.* **2014**, *24*, 6280–6290; d) Y. Yuetao, S. Qingde, Z. Guiwen, *Spectrochim. Acta Part A* **1999**, *55*, 1527–1533.
[17] C. Schoo, S. Bestgen, M. Schmidt, S. N. Konchenko, M. Scheer, P. W. Roesky, *Chem. Commun.* **2016**, *52*, 13217–13220.
[18] L. R. Morss, *Chem. Rev.* **1976**, *76*, 827–841.
[19] F. H. Allen, O. Kennard, D. G. Watson, L. Brammer, A. G. Orpen, R. Taylor, *J. Chem. Soc., Perkin Trans. 2* **1987**, S1–S19.
[20] a) C. M. Kotyk, M. E. Fieser, C. T. Palumbo, J. W. Ziller, L. E. Darago, J. R. Long, F. Furche, W. J. Evans, *Chem. Sci.* **2015**, *6*, 7267–7273; b) W. Huang, F. Dulong, T. Wu, S. I. Khan, J. T. Miller, T. Cantat, P. L. Diaconescu, *Nat. Commun.* **2013**, *4*, 1448.
[21] Z. Xie, K. Chui, Z. Liu, F. Xue, Z. Zhang, T. C. W. Mak, J. Sun, *J. Organomet. Chem.* **1997**, *549*, 239–244.
[22] a) M. C. Cassani, Y. K. Gun'ko, P. B. Hitchcock, M. F. Lappert, *Chem. Commun.* **1996**, 1987–1988; b) M. C. Cassani, Y. K. Gun'ko, P. B. Hitchcock, M. F. Lappert, F. Laschi, *Organometallics* **1999**, *18*, 5539–5547.
[23] E.-M. Schnöckelborg, J. J. Weigand, R. Wolf, *Angew. Chem. Int. Ed.* **2011**, *50*, 6657–6660; *Angew. Chem.* **2011**, *123*, 6787–6790.
[24] H. G. Von Schnering, W. Hoenle, *Chem. Rev.* **1988**, *88*, 243–273.
[25] M. Baudler, S. Akpapoglou, D. Ouzounis, F. Wasgestian, B. Meinigke, H. Budzikiewicz, H. Münster, *Angew. Chem. Int. Ed. Engl.* **1988**, *27*, 280–281; *Angew. Chem.* **1988**, *100*, 288–289.
[26] D. M. Sherman, T. D. Waite, D. M. Sherman, *Am. Mineral.* **1985**, *70*, 1262–1269.
[27] A. Pilon, P. Gírio, G. Nogueira, F. Avecilla, H. Adams, J. Lorenzo, M. H. Garcia, A. Valente, *J. Organomet. Chem.* **2017**, *852*, 34–42.
[28] a) M. H. V. Werts, R. T. F. Jukes, J. W. Verhoeven, *Phys. Chem. Chem. Phys.* **2002**, *4*, 1542–1548; b) W. M. Faustino, O. L. Malta, G. F. de Sá, *J. Chem. Phys.* **2005**, *122*, 054109.
[29] a) J. Kiwi, N. Denisov, Y. Gak, N. Ovanesyan, P. A. Buffat, E. Suvorova, F. Gostev, A. Titov, O. Sarkisov, P. Albers, V. Nadtochenko, *Langmuir* **2002**, *18*, 9054–9066; b) H. M. Fan, G. J. You, Y. Li, Z. Zheng, H. R. Tan, Z. X. Shen, S. H. Tang, Y. P. Feng, *J. Phys. Chem. C* **2009**, *113*, 9928–9935.
[30] S. Baskoutas, A. F. Terzis, *J. Appl. Phys.* **2006**, *99*, 013708.

[31] A. G. Joly, J. R. Williams, S. A. Chambers, G. Xiong, W. P. Hess, D. M. Laman, *J. Appl. Phys.* **2006**, *99*, 053521.
[32] N. C. Michenfelder, C. Gienger, A. Schnepf, A.-N. Unterreiner, *Dalton Trans.* **2019**, *48*, 15577–15582.
[33] W. Kaim, S. Ernst, S. Kohlmann, *Chem. Unserer Zeit* **1987**, *21*, 50–58.
[34] B. E. Bursten, M. L. Drummond, J. Li, *Faraday Discuss.* **2003**, *124*, 1–24.
[35] G. A. Salmon, W. A. Seddon, J. W. Fletcher, *Can. J. Chem.* **1974**, *52*, 3259–3268.
[36] F. Y. Jou, L. M. Dorfman, *J. Chem. Phys.* **1973**, *58*, 4715–4723.
[37] W. C. Martin, L. Hagan, J. Reader, J. Sugar, *J. Phys. Chem. Ref. Data* **1974**, *3*, 771–780.
[38] a) N. C. Jeong, J. S. Lee, E. L. Tae, Y. J. Lee, K. B. Yoon, *Angew. Chem. Int. Ed.* **2008**, *47*, 10128–10132; *Angew. Chem.* **2008**, *120*, 10282–10286; b) D. Xue, S. Zuo, H. Ratajczak, *Phys. B* **2004**, *352*, 99–104; *Angew. Chem.* **2008**, *120*, 10282–10286; *Angew. Chem. Int. Ed.* **2008**, *47*, 10128–10132.

Manuscript received: February 16, 2021
Accepted manuscript online: March 29, 2021
Version of record online: May 3, 2021

